

Alma Mater Studiorum Università di Bologna
Archivio istituzionale della ricerca

Spatio-temporal regression on compositional covariates: modeling vegetation in a gypsum outcrop

This is the final peer-reviewed author's accepted manuscript (postprint) of the following publication:

Published Version:

Bruno, F., Greco, F.P., Ventrucci, M. (2015). Spatio-temporal regression on compositional covariates: modeling vegetation in a gypsum outcrop. ENVIRONMENTAL AND ECOLOGICAL STATISTICS, 22(3), 445-463 [10.1007/s10651-014-0305-4].

Availability:

This version is available at: <https://hdl.handle.net/11585/372118> since: 2016-11-30

Published:

DOI: <http://doi.org/10.1007/s10651-014-0305-4>

Terms of use:

Some rights reserved. The terms and conditions for the reuse of this version of the manuscript are specified in the publishing policy. For all terms of use and more information see the publisher's website.

This item was downloaded from IRIS Università di Bologna (<https://cris.unibo.it/>).
When citing, please refer to the published version.

(Article begins on next page)

This is the final peer-reviewed accepted manuscript of:

Bruno, F., Greco, F. & Ventrucci, M. Spatio-temporal regression on compositional covariates: modeling vegetation in a gypsum outcrop. Environ Ecol Stat 22, 445–463 (2015). <https://doi.org/10.1007/s10651-014-0305-4>

The final published version is available online at: <https://doi.org/10.1007/s10651-014-0305-4>

Rights / License:

The terms and conditions for the reuse of this version of the manuscript are specified in the publishing policy. For all terms of use and more information see the publisher's website.

This item was downloaded from IRIS Università di Bologna (<https://cris.unibo.it/>)

When citing, please refer to the published version.

1 SPATIO-TEMPORAL REGRESSION ON COMPOSITIONAL COVARIATES:

2 MODELING VEGETATION IN A GYPSUM OUTCROP

3
4 **Francesca Bruno, Fedele Greco, Massimo Ventrucchi**

5 Dipartimento di Scienze Statistiche “P. Fortunati”,

6 University of Bologna, Italy

7
8 SUMMARY

9 Investigating the relationship between vegetation cover and substrate typologies is important for habitat
10 conservation. To study these relationships, common practice in modern ecological surveys is to collect
11 information regarding vegetation cover and substrate typology over fine regular lattices, as derived from
12 digital ground photos. Information on substrate typologies is often available as compositional measures,
13 e.g., the area proportion occupied by a certain substrate. Two primary issues are of interest for ecologists:
14 first, how much substrate typologies differ in terms of relative suitability for vegetation cover and,
15 second, whether suitability varies over time. This paper develops a novel procedure for managing
16 compositional covariates within a Bayesian hierarchical framework to effectively address the
17 aforementioned issues. A spatio-temporal model is adopted to estimate the temporal pattern
18 characterizing substrate relative suitability for vegetation cover and, at the same time, to account for
19 spatio-temporal correlation. Relative suitability is modeled by time-varying regression coefficients, and
20 spatial, temporal and spatio-temporal random effects are modeled using Gaussian Markov Random Field
21 models.

22
23 **KEYWORDS:** binomial data; compositional covariates; Intrinsic Gaussian Markov
24 Random Fields; hierarchical Bayesian model; vegetation cover; suitability

In ecological applications, over the past years, there has been an increasing interest in collecting and analyzing datasets with both spatial and temporal dimensions. The increasing use of imaging tools able to collect and process digital ground photos managed by Geographic Information System (GIS) (Bennett et al. 2000; Richardson et al. 2001; Booth et al. 2005) has introduced ecologists to a new framework in which the analysis of ecological outcomes, such as species richness, abundance and vegetation cover, is based on high-resolution spatially referenced data. Vegetation cover is one of the most important indicators of rangeland condition and plays a key role in habitat management and conservation policies (Booth and Tuller 2003).

In this paper, we investigate the relationship between vegetation cover and substrate typologies within a rupicolous basophilic habitat defined as priority by the European Commission (Council Directive 92/43/CEE). Available data consist of post-processed ground photos taken at several points throughout the study period, which provide information about vegetation cover and substrate typology in a fine regular lattice.

Modeling vegetation cover in terms of substrate typologies is crucial to evaluating substrate suitability, i.e., substrates' natural ability to support vegetation. Knowledge concerning substrate suitability is strategic in predicting future developments and reactions to possible environmental changes in the considered habitat. The ecological behavior of vegetation in arid and rocky environments has been investigated in several studies (Kuntz and Larson 2006; Pueyo and Alados 2007).

Regression models, often including spatio-temporal components, have been largely adopted in the ecological literature to investigate the relationships between ecological outcomes and environmental factors (Guisan and Zimmermann 2000; Fortin et al. 2012;

Kneib et al. 2008). A flexible framework for ecological data is represented by hierarchical Bayesian models (Wikle 2003). The hierarchical structure is useful for accounting for multiple sources of uncertainty and allows for model complexity to be handled in a suitable manner, namely by factorizing the joint distribution into simple conditional models. The role of hierarchical modeling in ecological studies has been discussed in Latimer et al. (2006).

In this paper, a hierarchical Bayesian approach is adopted to investigate the temporal pattern of substrate suitability for vegetation, considering four types of substrate that are found in the habitat under examination, namely moss, litter, soil and bare rock. To properly capture substrate suitability, spatio-temporal correlation must be taken into account: when handling lattice data, Gaussian Markov Random Fields (GMRFs, Rue and Held 2005) are popular tools for modeling structured effects in space and time or both.

A peculiar feature of the case study is that data concerning substrate typology are compositional, i.e., at a given time, substrate data are expressed as the proportion of cell grid occupied by each type of substrate. The compositional nature of substrate information implies an additional challenge for statistical modeling: regression on compositional covariates requires suitable techniques to obtain meaningful regression coefficients indicating the effect of each single compositional part. Analyses involving compositional data begin by mapping the compositional values belonging to the simplex onto real space by any of several possible transformations (Aitchison 1986; Egozcue and Pawlowsky-Glahn 2006). A popular transformation for compositional data is the isometric log-ratio (*ilr*) transformation (Egozcue et al. 2003), which has the advantage of isolating the contribution of a given compositional part with respect to all others. In the context of linear regression on compositional covariates, *ilr* transformation was

adopted by Hron et al. (2012), who proposed an inferential procedure that requires the estimation of as many models as the number of compositions.

In the present paper, starting from the proposal of Hron et al. (2012), a new approach for handling compositional covariates in regression models is developed within a Bayesian hierarchical framework. The proposed strategy provides regression coefficients that are easy to interpret as relative suitability values.

This paper is organized as follows. A motivating example describing the structure of the data concerning an ecological application is outlined in section 2. In section 3, the modeling approach is discussed, and the procedure for handling compositional covariates is proposed. The application results are discussed in section 4. The concluding remarks are provided in section 5.

2 MOTIVATING EXAMPLE

Our focus is on a study designed within the framework of the priority defined by the European Commission (Council Directive 92/43/CEE), with the aim of investigating habitat “6110* Rupicolous calcareous or basophilic grasslands of the *Alyso-Sedion albi*”. A sampling campaign was performed on a gypsum outcrop within the Site of Community Importance “IT4050001 Gessi Bolognesi e Calanchi dell’Abbadessa” located in the Emilia Romagna Region, Italy. For a detailed description of the case study, see Velli (2014).

Data were collected over a study period going from April 2012 to late March 2013. Sampling campaigns were adjourned during the dryness period of August and September, when low vegetation cover is expected, and on January because of snow cover. A total of nine sampling campaigns were conducted at unequally spaced times,

denoted as $t = 1, \dots, 9$. The study area consists of a $1.5 \times 1.5m$ *quadrat*, structured as a regular lattice of dimension 30×30 , containing 900 grid cells, indexed by $s = 1, \dots, 900$, which are denoted as *plots* in the ecological literature . At each time, a ground-photo of the study area was taken and then processed via GIS algorithms to produce a digital image for vegetation cover and ground composition. Namely, ground composition considers $D = 4$ substrates: *moss*, *litter*, *soil* and *bare rock*. . Each grid cell (plot) in the digital image provides information collected over $n = 100$ pixels. At time t and plot s , the number of pixels covered by a plant is denoted as y_{st} , and the proportions of substrate typologies are collected in the vector $\mathbf{z}_{st} = (z_{1st}, z_{2st}, z_{3st}, z_{4st})$. As an example, z_{1st} is the count, or the proportion, of pixels covered by moss in plot s at time t ; analogously we obtain the substrate proportions for litter (z_{2st}), soil (z_{3st}) and bare rock (z_{4st}). It is worth noticing that, at any time t and plot s , $z_{1st} + z_{2st} + z_{3st} + z_{4st} = n$, thus substrate typology \mathbf{z}_{st} is a compositional variable.

Some descriptive statistics concerning pixel-specific vegetation cover (expressed as y_{st}/n) are summarized in Table 1, where means and quartiles over the study area are reported for each time.

<i>T</i>	1	2	3	4	5	6	7	8	9
Mean	0.158	0.127	0.102	0.046	0.195	0.258	0.338	0.340	0.393
Q1	0.010	0.000	0.000	0.000	0.000	0.000	0.040	0.060	0.110
Median	0.060	0.040	0.000	0.000	0.080	0.140	0.210	0.220	0.310
Q3	0.210	0.150	0.110	0.000	0.310	0.420	0.600	0.560	0.640
Moran's I	0.433	0.569	0.510	0.469	0.534	0.600	0.612	0.615	0.614

Table 1 Descriptive statistics of vegetation cover (y_{st}/n) over time

The average vegetation cover changes substantially across time. A decreasing trend is observed until $t = 4$; at the fourth time point, vegetation is almost absent, later it

increases in terms of both the number of pixels where vegetation is present (i.e., Q1 is greater than zero only for $t \geq 7$) and average coverage. Last row in Table 1 reports the Moran's I statistics measuring spatial correlation. Moran's I index (Moran 1948) measures the degree of correlation between observations at neighboring plots. This index takes continuous values from -1 (maximum negative spatial correlation) to 1 (maximum positive spatial correlation) with 0 indicating absence of spatial correlation. A spatio-temporal representation of the vegetation cover is reported by maps in Figure 1. The spatial correlation characterizing the vegetation cover measured at the pixel level is considerable throughout the entire study period and becomes more evident from the fifth to the last time point, as evidenced by the Moran's I values in Table 1. Overall, the data show both spatial and temporal correlation.

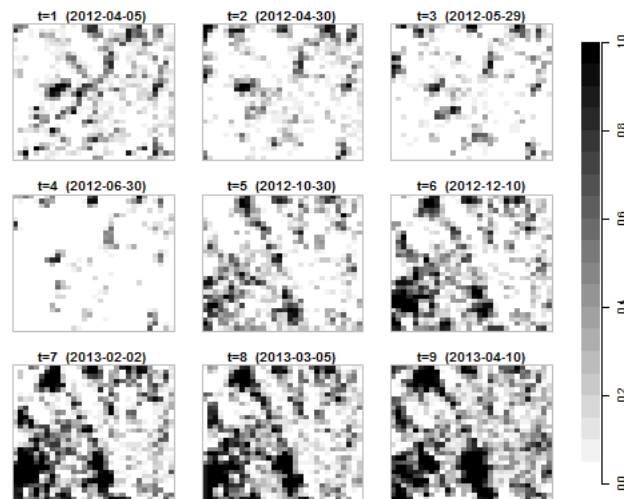


Fig. 1 Maps of vegetation cover at each collection time (indicated within brackets)

In Table 2, the pixel-specific shares z_{st} of substrate typologies are summarized, demonstrating the existence of temporal variability both within and between substrates.

<i>T</i>	1	2	3	4	5	6	7	8	9
Moss	0.46	0.30	0.35	0.35	0.42	0.50	0.57	0.54	0.49
Litter	0.29	0.15	0.14	0.19	0.06	0.01	0.03	0.01	0.01
Soil	0.09	0.30	0.26	0.14	0.22	0.23	0.17	0.20	0.18
Bare rock	0.16	0.25	0.25	0.32	0.30	0.26	0.23	0.25	0.32

Table 2 Share of substrate typology averaged over the study region at each collection time

To investigate the effect of substrate typology on vegetation cover, the marginal average cover over time (see the first row of Table 1) is considered as a benchmark to be compared to the substrate-specific conditional average. These syntheses are shown in the four panels of Figure 2 as solid and dashed lines, respectively. Noisy behavior characterizes the pattern observed on litter substrates, particularly at the end of the study period, when such a typology is scarcely represented in the region (see Table 2). Vegetation cover on moss, soil and bare rock substrates shows a decreasing trend until summer, followed by an increasing trend; such a pattern reflects the general behavior of vegetation over the study period due to the natural vegetation life cycle in dry grasslands.

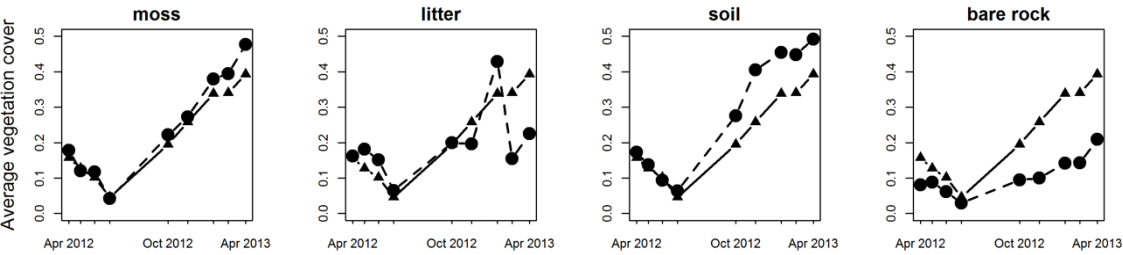


Fig. 2 Comparison of trends for average vegetation cover (solid line) and conditional vegetation cover (dashed lines) for each substrate

The aim of the model proposed in the following section is both to capture the marginal temporal trend for vegetation, basically due to climate, and to quantify the substrate-specific effect on vegetation, i.e., the ability of a substrate typology to favor/inhibit vegetation cover . Because of the compositional nature of the substrate data, such an ability can only be evaluated comparatively among substrates. In fact, if a substrate typology shows a higher-than-average vegetation cover, necessarily some other substrates will show lower-than-average cover; for this reason, substrate effects will be interpreted as “relative suitability” measures. Two main questions arise: How much do substrate typologies differ in terms of relative suitability? Does this difference vary over time? From a statistical point of view, substrate suitability estimates can be obtained as regression coefficient estimates of a regression model where vegetation cover is the response variable and substrate typology is aa compositional covariate. A spatio-temporal modelling framework is seek in this work for two reasons. First, spatial and temporal dependencies observed in the descriptive plots for vegetation cover need to be modelled for reliable estimates of the regression coefficients to be obtained (ref?). Second, it is of interest to model the temporal structure in the regression coefficients to predict suitability of all substrates at unobserved times and investigate their temporal variations across the study period.

3 MODEL

The relationship between substrate typology and vegetation cover is modeled by the hierarchical Bayesian model described in what follows; the strategy for handling compositional covariates is discussed in the next subsection. Let y_{st} denote the count of

pixels covered by vegetation at plot s and time t . Conditional on the vegetation occupancy probability π_{st} , counts are assumed to follow a Binomial distribution, i.e., the binary response at each pixel within a plot is considered as the realization of an independent trial. Spatio-temporal variability and dependence on covariates are managed at higher levels of the hierarchy. The likelihood is specified as follows:

$$y_{st} | \pi_{st} \sim \text{Binomial}(\pi_{st}, n) \quad s = 1, \dots, S; t = 1, \dots, T$$

where n denotes the constant number of pixels belonging to each plot. The model can be easily generalized to the case of a variable number of trials; nevertheless, having a constant number of trials simplifies the algebraic representation of the model presented in section 3.2 and in Appendix A. To model the vegetation occupancy probability as a function of covariates, we adopt the *probit* link; the linear predictor is specified as follows:

$$\Phi^{-1}(\pi_{st}) = \eta_{st} = \mathbf{x}_{st}' \boldsymbol{\beta}_t + \alpha_t + \theta_s + \delta_{st} \quad s = 1, \dots, S; t = 1, \dots, T \quad (0)$$

where \mathbf{x}_{st} is a P -dimensional covariate vector and $\boldsymbol{\beta}_t = (\beta_{1t}, \dots, \beta_{pt}, \dots, \beta_{Pt})$ denotes the vector of time-varying regression coefficients. Postulating time-varying coefficients implies that time is an effect modifier; checking this assumption in our case study is crucial because the aim is to evaluate the evolution (if any) of substrate suitability over time. Three sets of random effects are included to account for spatio-temporal variability not explained by the dependence on the covariates: $\boldsymbol{\alpha} = (\alpha_1, \dots, \alpha_t, \dots, \alpha_T)$ and

208 $\boldsymbol{\theta} = (\theta_1, \dots, \theta_s, \dots, \theta_S)$ are vectors of temporal and spatial main effects, respectively,

209 whereas vector $\boldsymbol{\delta} = (\delta_{11}, \dots, \delta_{st}, \dots, \delta_{ST})$ contains space-time interactions.

210 Modeling of both regression coefficients and random effects is based on the theory
 211 concerning Intrinsic Gaussian Markov Random Fields (IGMRFs, see Rue and Held
 212 2005, for a comprehensive review), which are very popular tools for spatio-temporal
 213 modeling of lattice data. Because of the Markov property, which implies the sparseness
 214 of the precision matrix, IGMRFs allow for extremely fast computations. IGMRFs have
 215 also been extended to cope with irregularly spaced time locations by Lindgren and Rue
 216 (2008); this is particularly useful in our case study, in which measurements have been
 217 collected at unequally spaced times, as often occurs in ecological studies.

218 In the following, $IGMRF_J(\tau \mathbf{K})$ denotes the (multivariate normal) distribution of a J -
 219 dimensional random vector with $J \times J$ -dimensional structure matrix \mathbf{K} and precision
 220 parameter τ ; the IGMRFs are improper, i.e., \mathbf{K} is rank-deficient. Structure matrix \mathbf{K}
 221 describes conditional dependence relationships derived from assumptions concerning
 222 the spatial and temporal structure of the phenomenon.

223 Let $\boldsymbol{\beta}_p = (\beta_{p1}, \dots, \beta_{pt}, \dots, \beta_{pT})$ denote the T -dimensional vector of regression coefficients
 224 referring to the p -th covariate obtained by re-arranging the p -th elements of vectors

225 $\boldsymbol{\beta}_t = (\beta_{1t}, \dots, \beta_{pt}, \dots, \beta_{Pt})$ for all $t = 1, \dots, T$. We introduce a temporal dependence among
 226 these coefficients, assuming a smooth variation of the covariate effect over the study

227 period, by specifying the prior $\boldsymbol{\beta}_p \sim IGMRF_T(\tau_{\beta_p} \mathbf{K}_{\beta_p})$; $p = 1, \dots, P$. Following the
 228 modeling strategy first proposed in Knorr-Held (2000) in the context of spatio-temporal
 229 disease mapping, prior distributions for spatio-temporal random effects are specified as
 230 follows: $\boldsymbol{\alpha} \sim IGMRF_T(\tau_{\alpha} \mathbf{K}_{\alpha})$, $\boldsymbol{\theta} \sim IGMRF_S(\tau_{\theta} \mathbf{K}_{\theta})$ and $\boldsymbol{\delta} \sim IGMRF_{ST}(\tau_{\delta} \mathbf{K}_{\delta})$.

231 Structure matrices \mathbf{K}_{β_p} and \mathbf{K}_α need to be specified to capture a smooth temporal
 232 behavior. In this context, Random Walk (RW) priors (i.e., IGMRFs on the line) of order
 233 1 is a popular choice; we set common temporal structure matrices $\mathbf{K}_{\beta_p} = \mathbf{K}_\alpha = \mathbf{K}_{RW}$. It
 234 follows that $\text{rank}(\mathbf{K}_{RW}) = T - 1$. Because our data are irregularly spaced over time, the
 235 structure matrix typically used for this process must be adapted. To this aim, Rue and
 236 Held (2005) propose a solution by considering the integration of the Wiener process
 237 (Wahba, 1978).

238 Structure matrix \mathbf{K}_θ is specified as the $S \times S$ -dimensional Laplacian matrix of the
 239 graph induced by a first-order neighboring structure on the regular lattice formed by the
 240 plots. The i -th diagonal entry is equal to the number of neighbors of plot i , whereas the
 241 ij -th entry equals -1 iff plots i and j share a common boundary and zero otherwise. With
 242 this specification, $\text{rank}(\mathbf{K}_\theta) = S - 1$.

243 Regarding the spatio-temporal interaction term, four types of interactions are envisioned
 244 in Knorr-Held (2000), leading to different structure matrices \mathbf{K}_δ obtained as a
 245 Kronecker product of temporal and spatial structure matrices $\mathbf{K}_\delta = \mathbf{K}_{time} \otimes \mathbf{K}_{space}$.
 246 Specifying $\mathbf{K}_\delta = \mathbf{I}_T \otimes \mathbf{I}_S$ corresponds to a Type I interaction, in which independence
 247 among δ s is postulated; a Type II interaction, obtained by specifying the structure
 248 matrix as $\mathbf{K}_\delta = \mathbf{K}_{RW} \otimes \mathbf{I}_S$, is suitable if plots show different temporal trends with no
 249 structure in space; a Type III interaction, $\mathbf{K}_\delta = \mathbf{I}_T \otimes \mathbf{K}_\theta$, assumes different spatial trends
 250 with no structure in time. Finally, a Type IV interaction, $\mathbf{K}_\delta = \mathbf{K}_{RW} \otimes \mathbf{K}_\theta$, involves both
 251 a spatial and a temporal structure.

252 To ensure model identifiability, appropriate linear constraints need to be imposed on the
 253 spatial (θ) and spatio-temporal (δ) random effects, whereas the temporal random

effects (α) are unconstrained and can be considered time-dependent random intercepts. The number of linear constraints needed to ensure identifiability corresponds to the rank deficiency of the structure matrix of an IGMRF. As pointed out in Schrödle and Held (2011), identifiability can be ensured by computing the null space of the structure matrix and using the obtained eigenvectors as linear constraints. A simple sum-to-zero constraint is required for the identifiability of the spatial effects because $rank(\mathbf{K}_\theta) = S - 1$ (i.e., the null space of \mathbf{K}_θ is spanned by a constant vector). Because of the properties of the Kronecker product, the rank deficiency of \mathbf{K}_δ depends on the specified type of interaction: $rank(\mathbf{K}_\delta) = T \times S - rank(\mathbf{K}_{time}) \times rank(\mathbf{K}_{space})$; when a Type IV interaction is considered, the number of required linear constraints becomes extremely high when S and T are large.

Model hierarchy is completed by prior specification for precision parameters of the IGMRFs: we assume independent, small-parameter Gamma distributions both to preserve non-informativeness and to take advantage of the conjugacy between the Gaussian and the Gamma distribution in building the MCMC sampler.

3.1 Managing compositional covariates

As discussed in section 2, the main aim of this study is to investigate the effect of substrate typology on vegetation cover. Because at each plot substrate typology is expressed as a proportion, these explanatory variables need to be managed coherently with compositional algebra. For the sake of simplicity, in this section, spatio-temporal subscripts are dropped, and the focus is on a simple linear regression model; nevertheless, the developed theory can be readily applied to model (1).

278 Consider a D -dimensional vector of compositional covariates, $\mathbf{z} = (z_1, \dots, z_d, \dots, z_D)$, that
 279 can be represented with unit-sum constraint in the simplex
 280 $S^D = \left\{ \mathbf{z} = (z_1, \dots, z_d, \dots, z_D)' , z_d > 0, \sum_{d=1}^D z_d = 1 \right\}$. If untransformed compositional
 281 covariates are used, the design matrix of the proportional representation of compositions
 282 is singular due to the sum-to-one constraint. This issue can be addressed by a
 283 transformation that allows for a transition from the D -dimensional simplex to
 284 unconstrained $(D-1)$ -dimensional real space, \Re^{D-1} . In this paper, we adopt the *ilr*
 285 transformation (Egozcue et al., 2003), which is an isometry between S^D and \Re^{D-1} ,
 286 leading to *ilr*-transformed covariates $\mathbf{x} = \text{ilr}(\mathbf{z}) = (x_1, \dots, x_i, \dots, x_{D-1})'$. Following Egozcue
 287 et al. (2003), an orthonormal basis matrix \mathbf{B} associated with the coordinate system
 288 generated by $\text{ilr}(\mathbf{z})$ can be obtained by sequential binary partitioning. The i -th row of
 289 this matrix is

$$291 \quad \mathbf{b}_i = \sqrt{\frac{D-i}{D-i+1}} \left[\underbrace{0, \dots, 0}_{i-1 \text{ times}}, +1, \underbrace{-\left(D-i\right)^{-1}, \dots, -\left(D-i\right)^{-1}}_{D-i \text{ times}} \right]; \quad \mathbf{b}_i \in \Re^D; i = 1, \dots, D-1. \quad (0)$$

292
 293 The i -th component of the *ilr* coordinates vector \mathbf{x} is defined as

$$295 \quad x_i = \text{ilr}(\mathbf{z})_i = \sqrt{\frac{D-i}{D-i+1}} \ln \frac{z_i}{\sqrt[D-i]{\prod_{j=i+1}^D z_j}} \quad \text{for } i = 1, \dots, D-1. \quad (0)$$

296
 297 In the context of compositional data analysis, other widely used transformations include
 298 the centered log-ratio (*clr*) and the additive log-ratio (*alr*) transformations. The *alr*

transformation raises several issues in terms of interpretability because it is not an isometric transformation. According to Tolosana-Delgado and Van Den Boogaart (2013), the *clr* representation of a composition is often convenient in a regression framework because each coefficient can be related to an original component. Nonetheless, the *clr* is not expressed in terms of an orthogonal basis, neither of the simplex nor of the real space and it generates a singular design matrix that requires a sum-to-zero constraint for estimation of the regression coefficients. In a simple linear regression framework, this does not raise particular issues, since estimation of the regression coefficients is obtained by computing the Moore-Penrose inverse. This is not practical in models where regression coefficients are modelled along time, as in our application, since time-specific constraints would result in considerable computational burden. Hence, our strategy for regression on compositional covariates consists in estimating the model with *ilr* coordinates and in obtaining the *clr* coefficients by exploiting the relationship between *ilr* and *clr* coordinates.

The *ilr* transformation is directly associated with orthogonal coordinates in the simplex (Egozcue et al. 2003). The first component of the *ilr*-transformed vector is defined as a function of the ratio between z_1 and the geometric mean of *all* of the remaining components of \mathbf{z} . Thus, when *ilr*-transformed covariates, \mathbf{X} , are introduced into the linear model $\mathbf{y} = \alpha + \mathbf{X}\boldsymbol{\beta} + \boldsymbol{\varepsilon}$, the first regression coefficient, β_1 , is directly interpreted as the *relative* effect of part 1; namely, it is the expected increment of the response variable when the first part increases its relative weight with respect to an average of all the other parts. The other regression coefficients cannot be interpreted analogously, nonetheless, as will be discussed in the following, meaningful regression coefficients for all parts can be obtained by switching from *ilr* to *clr* coefficients by a simple linear transformation exploiting the relationship between *ilr* and *clr* coordinates.

324 The orthonormal basis B introduced in equation (XX) allows to switch from *ilr* to *clr*
 325 coordinates by the linear transformation $\tilde{x} = clr(z) = ilr(z)' B = x' B$.

326 The model fit is not sensitive to the chosen transformation, i.e., the models
 327 $y = \alpha + X\beta + \varepsilon$ and $y = \alpha + \tilde{X}\tilde{\beta} + \varepsilon$, based respectively on *ilr* and *clr* transformed
 328 covariates, deliver the same fit and the same estimate of the intercept, in fact the two
 329 models have the same hat matrix:

330

$$331 \quad \tilde{X}(\tilde{X}'\tilde{X})^{-}\tilde{X} = XB(B'X'XB)^{-}B'X' = X(X'X)^{-1}X'$$

332

333 since $(B'X'XB)^{-} = B'(X'X)^{-1}B$ and $B'B = I$, where A^{-} denotes the Moore-penrose
 334 generalized inverse of A . Eventually, *clr* coefficients can be obtained by means of the
 335 transformation $\tilde{\beta} = B\beta$.

336

337 Vector $\tilde{\beta}$ should be considered as the key parameter in the context of regression on
 338 compositional covariates. Indeed, the vector contains all the relevant information
 339 concerning the effect of each part on the response variable. A remarkable feature of $\tilde{\beta}$
 340 is that

341

$$342 \quad I_D'\tilde{\beta} = \sum_{d=1}^D \tilde{\beta}_d = 0 \tag{0}$$

343

344 holds by construction. Relationship (0) demonstrates an intuitive dependence structure
 345 characterizing $\tilde{\beta}$ that is readily interpretable and particularly appealing in the context of
 346 regression on compositional covariates. For further illustration, consider an obvious

feature of compositional data: if the proportion of part d increases, then the proportion of at least one of the other parts must decrease because of the sum-to-one constraint. Thus, if increasing the share of the d -th part does have a positive effect on the response variable, then increasing the share of some other part will necessarily have a negative effect. For this reason, we interpret $\tilde{\boldsymbol{\beta}}$ coefficients as “relative effects” of a part w.r.t. all of the others.

Referring to model (1), the set of compositional covariates \mathbf{z}_{st} at plot s and time t is included in the linear predictor after *ilr* transformation as $\mathbf{x}_{st} = \text{ilr}(\mathbf{z}_{st})$, i.e., $\Phi^{-1}(\pi_{st}) = \mathbf{x}_{st}'\boldsymbol{\beta}_t + \alpha_t + \theta_s + \delta_{st}$; hence, model (1) contains $P = D - 1$ regressors.

3.2 Computational details

As is typical in complex hierarchical Bayesian models, the joint posterior distribution is not available in closed form and needs to be approximated. The Markov property of IGMRF models implies sparseness of the precision structure matrix, which allows fast computations, making spatio-temporal modeling with a large amount of lattice data feasible. Two alternative strategies are currently very popular for approximating the joint posterior distribution: MCMC sampling and Integrated Nested Laplace Approximations (INLA, Rue and Martino 2009). The latter is particularly suited for latent GMRF models and provides very accurate approximations of the posterior distribution. In addition, INLA definitely outperforms MCMC approaches in terms of computational time and for more precise approximations to be obtained. Thus, such a method appears to be preferable and should be used whenever possible. INLA has been made easily implementable by the R package INLA (Rue et al. 2013). The problem with

applying INLA to our case study is that, when a Type IV interaction is considered, the large number of linear constraints required for model identifiability makes the approach computationally unfeasible, causing computer crash.

For this reason, MCMC sampling is a necessary tool for the purpose of this paper. The MCMC algorithm has been implemented by adopting the popular auxiliary variable approach introduced in Albert and Chib (1993) and developed successively in several papers. This approach preserves full conditionals in GMRF form, which are lost in the case of non-normal likelihood: this is crucial for fast sampling. The approach based on data augmentation introduces, for each *Bernoulli* trial denoted by subscript i , in plot s at time t , the following auxiliary variables:

$$w_{ist} \sim N(\mathbf{x}_{st}'\boldsymbol{\beta}_t + \alpha_t + \theta_s + \delta_{st}, 1) \quad i = 1, \dots, n; \quad s = 1, \dots, S; \quad t = 1, \dots, T$$

The Binomial likelihood is retrieved by specifying

$$\tilde{y}_{ist} = \begin{cases} 1 & \text{if } w_{ist} > 0 \\ 0 & \text{if } w_{ist} \leq 0 \end{cases} \quad \sum_i \tilde{y}_{ist} = y_{st}$$

where $\tilde{y}_{ist} = 1$ and $\tilde{y}_{ist} = 0$ appear y_{st} and $n - y_{st}$ times, respectively. It follows that the full conditional distributions of the auxiliary variables are truncated Normal:

$$w_{ist} | \dots \sim \begin{cases} N(\mathbf{x}_{st}'\boldsymbol{\beta}_t + \alpha_t + \theta_s + \delta_{st}, 1) I(w_{ist} > 0) & \text{if } \tilde{y}_{ist} = 1 \\ N(\mathbf{x}_{st}'\boldsymbol{\beta}_t + \alpha_t + \theta_s + \delta_{st}, 1) I(w_{ist} \leq 0) & \text{if } \tilde{y}_{ist} = 0 \end{cases} \quad (0)$$

393 Summing over the pixels, we obtain $w_{\bullet st} = \sum_{i=1}^n w_{ist}$. Conditionally on $w_{\bullet st}$, MCMC

394 sampling can proceed as in a standard Bayesian linear model, where $w_{\bullet st}$ serves as

395 pseudo-data. The linear predictor can be written in compact form as follows:

396

$$397 \quad \mathbf{w}_{\bullet} = \mathbf{X}'\boldsymbol{\beta} + \boldsymbol{\alpha} \otimes \mathbf{I}_S + \mathbf{I}_T \otimes \boldsymbol{\theta} + \boldsymbol{\delta}$$

398

399 where \mathbf{I}_k denotes a k -dimensional unit vector, $\mathbf{X} = \text{diag}(\mathbf{X}_1, \dots, \mathbf{X}_t, \dots, \mathbf{X}_T)$ is the

400 $ST \times T(D-1)$ -dimensional block-diagonal matrix with $S \times (D-1)$ -dimensional blocks

401 \mathbf{X}_t containing *ilr*-transformed covariates at time t and $\boldsymbol{\beta} = (\boldsymbol{\beta}_1, \dots, \boldsymbol{\beta}_t, \dots, \boldsymbol{\beta}_T)$ is the

402 $(D-1)T$ -dimensional vector of time-varying coefficients.

403 In the context of the Bayesian linear regression model, implementing a Gibbs sampler

404 involves standard MCMC tools; it is worth noting that sampling under linear constraints

405 for the interaction term, even for a Type IV interaction model, is not an hard task. In

406 fact, it can be shown that the null space spanned by the eigenvectors associated with

407 null eigenvalues of the structure matrix \mathbf{K}_{δ} is equivalent to the null space spanned by

408 the eigenvectors associated with null eigenvalues of the Kronecker product $\mathbf{C}_S \otimes \mathbf{C}_T$,

409 where \mathbf{C}_k denotes the k -dimensional centering matrix. Therefore, samples from the full

410 conditional distribution of $\boldsymbol{\delta}$ can be obtained by centering samples over space and time

411 on the fly at each MCMC iteration. Full conditional distributions for all of the

412 parameters are reported in Appendix A.

413 Several further refinements to the Gibbs sampler built for our case study can be adopted

414 to improve the efficiency of the MCMC algorithm. Regarding the auxiliary variable

approach, Frühwirth-Schnatter et al. (2007) propose an augmented model with lower dimensionality, where the number of required latent variables per observation becomes independent of the number of trials. Furthermore, block-sampling has been shown to considerably improve the mixing of Markov chains when some parameters show high correlation. Nonetheless, we adopt a Gibbs sampler in our case study because it allows for accurate results to be obtained within a fairly reasonable computational time.

4 APPLICATION

4.1 Model selection

Starting from model (1), several specifications can be proposed, according to different assumptions regarding the effect of substrate typology and the structured spatio-temporal effects. Namely, we estimate and compare a total of 10 competing models: all of them include a pure temporal effect (i.e., α_t) and a pure spatial effect (i.e., θ_s). The models differ with respect to the spatio-temporal interaction type (I,II,III,IV); moreover substrate effect is specified either as constant or time-varying. All temporal effects are modeled as RW1 opportunely adapted for considering unequally spaced times. The models are compared in terms of the Deviance Information Criterion (DIC, Spiegelhalter et al. 2002) in Table 3.

	Interaction				
Substrate effect	Type 1	Type 2	Type 3	Type 4	No
Constant	33501	33518	33349	33510	188053
Time-varying	33496	33513	33343	33515	183137

Table 3 Deviance Information Criterion (DIC) corresponding to different model specifications for spatio-temporal interaction and substrate effect (time-constant or time-varying)

From the last column of this table, it can be observed that neglecting spatio-temporal interactions produces very poor performance. The selected model (whose DIC is reported in bold in the table) includes time-varying coefficients and a Type 3 interaction. The inclusion of a Type 4 interaction does not improve the model fit, regardless of the assumption made about substrate effects. Despite the small differences in terms of DIC exhibited by models with a Type 3 interaction, the results presented in the following section provide evidence of a significant change in the covariate effect over time, supporting the selection of the time-varying coefficient model. Ultimately, the selected model is:

$$y_{st} | \pi_{st} \sim \text{Binomial}(\pi_{st}, n) \quad s = 1, \dots, S; t = 1, \dots, T$$

$$\Phi^{-1}(\pi_{st}) = \mathbf{x}'_{st} \boldsymbol{\beta}_t + \alpha_t + \theta_s + \delta_{st} \quad \text{where } \boldsymbol{\beta}_t = (\beta_{1t}, \dots, \beta_{dt}, \dots, \beta_{(D-1)t})$$

$$\boldsymbol{\beta}_d = (\beta_{d1}, \dots, \beta_{dt}, \dots, \beta_{dT}) \sim \text{IGMRF}_T(\tau_{\beta_d} \mathbf{K}_{RW}); d = 1, \dots, D-1$$

$$\boldsymbol{\alpha} \sim \text{IGMRF}_T(\tau_{\alpha} \mathbf{K}_{RW}), \boldsymbol{\theta} \sim \text{IGMRF}_S(\tau_{\theta} \mathbf{K}_{\theta}); \boldsymbol{\delta} \sim \text{IGMRF}_{ST}(\tau_{\delta} \mathbf{K}_{\delta})$$

where $\mathbf{K}_{\delta} = \mathbf{I}_T \otimes \mathbf{K}_{\theta}$, in accordance with a Type III interaction. Because, as mentioned in section 3, vector $\boldsymbol{\alpha}$ is unconstrained in model estimation, this purely temporal effect is devoted to capture, in the *probit* scale, the natural vegetation life cycle.

4.2 Results

Results are obtained from a post-convergence MCMC sample of size 10,000 obtained by thinning a 100,000 sample to reduce correlation while guaranteeing an adequate effective sample size.

In the upper panels (a1-a3) of Figure 3, posterior distributions ($\beta_t | y$) of parameters $\beta_t = (\beta_{1t}, \dots, \beta_{dt}, \dots, \beta_{(D-1)t})$ are reported for $t = 9$ as an example. The lower panels (b1-b4) report posterior distributions of *clr*-regression coefficients $\tilde{\beta}_t$; these posterior distributions are obtained by transforming β_t at each MCMC iteration. Panels (a1) and (b1) contain the same information, up to a scaling constant relating $\beta_{1,9}$ and $\tilde{\beta}_{1,9}$. The positiveness of this coefficient implies that the first substrate typology (moss) encourages vegetation cover when compared with other substrates typologies, i.e., moss shows positive “relative suitability”. Panels (a2) and (a3) contain, respectively, the posterior distributions of $\beta_{2,9}$ and $\beta_{3,9}$: these parameters do not convey readily interpretable information concerning substrate suitability because, as discussed in section 3.1, they do not refer to any direct comparison between one compositional part and all others. As a consequence, testing for the nullity of these coefficients is pointless because a null coefficient does not directly imply a non-significant effect of some compositional part on the response variable. As a matter of fact, no sound considerations about the relative suitability of litter, soil and bare rock can be drawn from panels (a2) and (a3). On the other hand, panels (b2)-(b4) convey direct information about substrate relative suitability: the posterior distribution of regression coefficient associated with litter (panel b2) is centered at zero, meaning that litter shows average suitability, whereas soil (panel b3) and bare rock (panel b4) have positive and negative relative suitability, respectively.

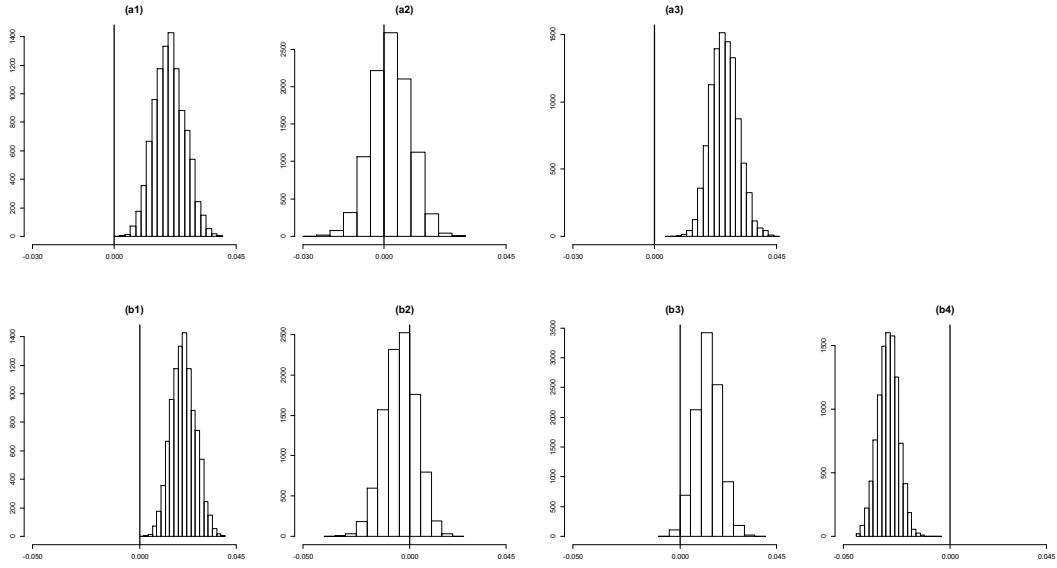


Fig. 3 Posterior distributions of the regression coefficients for the last collection time (panels a1-a3). Posterior distributions of transformed regression coefficients expressing the relative suitability for moss (b1), litter (b2), soil (b3) and bare rock (b4). Vertical lines correspond to zero

Because transformed coefficients are directly comparable, we provide some suggestions on how posterior estimates can be used to describe findings about substrate suitability. Upon first glance, at a given time, the substrates can be ordered from the most to the least suitable for vegetation cover based on the posterior means $E(\tilde{\beta}_{dt}|\mathbf{y})$: at time 9, moss turns out to be the most suitable substrate typology, followed by soil, litter and bare rock. Moreover, a rigorous comparison between the suitability of substrates d and d' that takes account of the uncertainty about parameter estimates can be obtained by evaluating $Pr(\tilde{\beta}_{dt} > \tilde{\beta}_{d't}|\mathbf{y})$, i.e., the posterior probability that the suitability of substrate d is higher than that of substrate d' . This task is easily addressed by exploiting the MCMC sample. It is observed that, at time 9, the posterior probabilities that moss is more suitable than litter, soil and bare rock are 0.98, 0.81 and 1, respectively.

Furthermore, it is interesting to determine whether the heterogeneity characterizing substrate suitability changes over time; it is worth noting that the more the estimated

coefficients at time t are dispersed around zero, the more the substrates show differences in terms of suitability. Thus, the posterior distribution $sd(\tilde{\beta}_t)|y$, $t=1,\dots,9$, gives information about the heterogeneity of substrates in terms of the suitability at each time. Figure 4 shows that the heterogeneity increases over the study period.

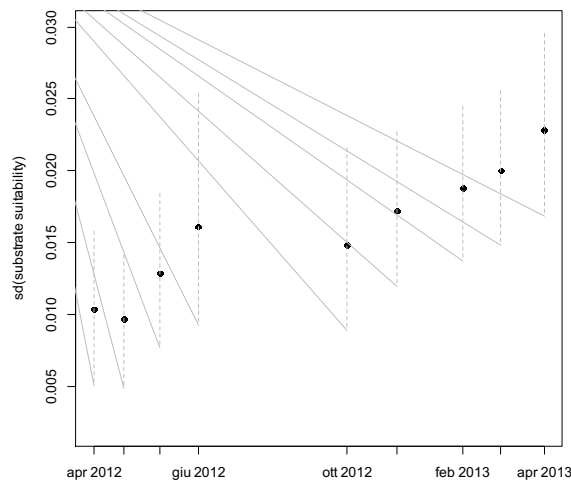


Fig. 4 Posterior distribution of $sd(\tilde{\beta}_t)|y$ over time

The biological motivation of this behavior can be found in the increase in vegetation cover, from October to the end of the study period, caused by a higher propensity of vegetation to occur in the substrates that exhibit greater availability of nutrient resources (i.e., moss and soil) than do the others (litter and bare rock). Finally, we describe findings about the temporal evolution of substrate relative suitability that are helpful in addressing the ecological questions posed at the end of section 2. In each panel of Figure 5, the posterior mean of $\tilde{\beta}_t$ at the collection times (filled circles), the predictions at unobserved times (black solid line) and credible bands

(grey dashed lines) are reported. Predictions are obtained via MCMC sampling from the posterior predictive distribution of $\tilde{\beta}_t$.

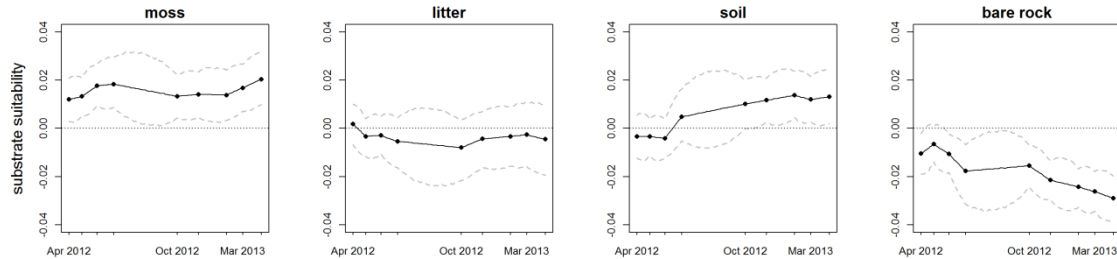


Fig. 5 Substrate relative suitability over time

Moss is revealed to be the most suitable substrate at the beginning of the study period, and its relative suitability remains nearly constant over time. On the other hand, the relative suitability of soil is approximately zero (i.e., approximately average) at the beginning and increases over time, reaching a positive relative suitability level in winter. The opposite behavior is exhibited by bare rock, which is less suitable than average and shows a decreasing pattern over time. Finally, litter presents constant average suitability over time.

It is worth noting that, in contrast to the results shown in Figure 2, where the temporal pattern of substrate-specific effects is confounded with the marginal trend for vegetation, the results shown in Figure 5 provide direct information on the relative suitability level of each substrate and how these levels vary over the study period, after properly accounting for spatial and temporal correlation. These results are in agreement with the ecological literature on this type of habitat (Lundholm 2003, Otsus and Zobel 2002) as stated in Velli (2014).

5. CONCLUSIONS

In this work, a spatio-temporal model for ecological data derived from digital ground photos is presented. The primary focus is on quantifying the relation between vegetation cover and substrate typology, expressed as compositional data, by accounting for spatial and temporal correlation. The proposed models include spatial, temporal and spatio-temporal effects modeled as IGMRFs. A novel approach for estimating the relative effect of compositional covariates on the response variable is developed within a Bayesian framework, through a procedure based on appropriate transformations of the regression coefficients. This procedure exploits the properties of the *ilr* transformation, which admits an orthonormal basis representation; this transformation allows for a transition between different coordinate systems, providing meaningful regression coefficients. In our opinion, the proposed approach constitutes a basis for future developments in such fields as non-linear and nonparametric regression for compositional covariates. To the best of our knowledge, these topics have been scarcely debated in the literature concerning both compositional data and Bayesian analysis.

The lattice structure of the data make GMRFs particularly suitable tools for modeling spatial and temporal dependence by specifying a conditional dependence structure. This ability allows for feasible computations that can be implemented both by the INLA approach and MCMC sampling; fast algorithms that allow for efficient sampling by exploiting the sparseness of the precision matrices are implemented within a Gibbs sampling scheme. Both the INLA and MCMC codes are available upon request from the corresponding author.

The model is applied to a dataset concerning a habitat included in the framework of the priority defined by the European Commission, where investigating the relationship

between vegetation cover and substrate typology can be helpful in quantifying substrate suitability. The case study demonstrates that the proposed modeling strategy produces valuable outcomes for ecologists. First, in ecological studies, knowledge of substrate suitability is strategic for habitat conservation, for instance, to predict future developments and reactions to possible environmental changes. Second, a modeling approach that is able to predict substrate suitability or other ecological responses over un-monitored periods of time is extremely useful in many common situations in which surveys cannot follow a regular plan, as in the case in which fieldwork activity is impossible because of adverse environmental and weather conditions.

One interesting ecological finding of the paper is that substrate relative suitability varies over time. A future line of research will focus on extending the proposed model to allow for smooth, rather than simply linear, effects of compositional covariates on ecological responses. Non-linear effects of substrate shares on ecological responses may often be observed, especially when the response of interest is a biodiversity index, such as species richness or evenness.

APPENDIX

The Gibbs sampler is implemented as follows:

1. Sample auxiliary variables from the truncated normal full conditionals (0).

Let \tilde{W} be the nST -dimensional vector of the auxiliary variables, full conditionals for the other parameters can be obtained as in the standard linear model with Gaussian likelihood, starting from the following expression of the linear predictor:

$$\begin{aligned}\tilde{\eta} &= (X \otimes I_n) \beta + (I_T \otimes I_S \otimes I_n) \alpha + (I_T \otimes I_S \otimes I_n) \theta + (I_T \otimes I_S \otimes I_n) \delta \\ &= \tilde{X} \beta + \tilde{A}_1 \alpha + \tilde{A}_2 \theta + \tilde{A}_3 \delta\end{aligned}$$

In what follows, the multivariate normal distribution is expressed in the canonical form (Rue and Held, 2005; page 27)

2. Sample the regression parameters from the distribution

$$\beta | \dots \sim N_C(\mathbf{b}_\beta, \mathbf{Q}_\beta)$$

$$\mathbf{b}_\beta = \tilde{X}' (\tilde{W} - \tilde{A}_1 \alpha - \tilde{A}_2 \theta - \tilde{A}_3 \delta) = n \tilde{X}' (\mathbf{w}_\bullet / n - (I_T \otimes I_S) \alpha - (I_T \otimes I_S) \theta - \delta);$$

$$\mathbf{Q}_\beta = \mathbf{P}_0 \Gamma_\beta \mathbf{P}_0' + \tilde{X}' \tilde{X} = \mathbf{P}_0 \Gamma_\beta \mathbf{P}_0' + n \tilde{X}' \tilde{X}$$

where $\Gamma_\beta = \text{diag}(\tau_{\beta_1}, \dots, \tau_{\beta_{D-1}}) \otimes \mathbf{K}_{RW}$ and \mathbf{P}_0 is a permutation matrix with the following

structure:

$$\mathbf{P}_0 = \begin{bmatrix} \mathbf{I}_{D-1} \otimes \mathbf{v}_1' \\ \dots \\ \mathbf{I}_{D-1} \otimes \mathbf{v}_t' \\ \dots \\ \mathbf{I}_{D-1} \otimes \mathbf{v}_T' \end{bmatrix}$$

The T -dimensional vector \mathbf{v}_t contains 1 at position t and zero elsewhere.

3. Sample the temporal effects, i.e., the time-varying intercepts, from the distribution

$$\alpha | \dots \sim N_C(\mathbf{b}_\alpha, \mathbf{Q}_\alpha)$$

$$\mathbf{b}_\alpha = \tilde{A}_1' (\tilde{W} - \tilde{X} \beta - \tilde{A}_2 \theta - \tilde{A}_3 \delta) = n \tilde{A}_1' (\mathbf{w}_\bullet / n - \tilde{X} \beta - (I_T \otimes I_S) \theta - \delta);$$

$$\mathbf{Q}_\alpha = \tau_\alpha \mathbf{K}_{RW} + \tilde{A}_1' \tilde{A}_1 = \tau_\alpha \mathbf{K}_{RW} + n \mathbf{S} \mathbf{I}_T$$

4. Sample the spatial effect from the distribution

$$\theta | \dots \sim N_C(\mathbf{b}_\theta, \mathbf{Q}_\theta)$$

$$\mathbf{b}_\theta = \tilde{\mathbf{A}}_2' (\tilde{\mathbf{W}} - \tilde{\mathbf{X}}\boldsymbol{\beta} - \tilde{\mathbf{A}}_1\boldsymbol{\alpha} - \tilde{\mathbf{A}}_3\boldsymbol{\delta}) = n(\mathbf{I}_T \otimes \mathbf{I}_S)' (\mathbf{w}_\bullet/n - \mathbf{X}\boldsymbol{\beta} - (\mathbf{I}_T \otimes \mathbf{I}_S)\boldsymbol{\alpha} - \boldsymbol{\delta});$$

$$\mathbf{Q}_\theta = \tau_\theta \mathbf{K}_\theta + \tilde{\mathbf{A}}_2' \tilde{\mathbf{A}}_2 = \tau_\theta \mathbf{K}_\theta + n \mathbf{I}_S$$

Centre the sampled values.

$$\tilde{\mathbf{X}}\boldsymbol{\beta} + \tilde{\mathbf{A}}_1\boldsymbol{\alpha} + \tilde{\mathbf{A}}_2\boldsymbol{\theta} + \tilde{\mathbf{A}}_3\boldsymbol{\delta}$$

5. Sample the spatiotemporal random effects from the distribution

$$\boldsymbol{\delta} | \dots \sim N_C(\mathbf{b}_\delta, \mathbf{Q}_\delta)$$

$$\mathbf{b}_\delta = (\tilde{\mathbf{W}} - \tilde{\mathbf{X}}\boldsymbol{\beta} - \tilde{\mathbf{A}}_1\boldsymbol{\alpha} - \tilde{\mathbf{A}}_2\boldsymbol{\theta}) = n(\mathbf{w}_\bullet/n - \mathbf{X}\boldsymbol{\beta} - (\mathbf{I}_T \otimes \mathbf{I}_S)\boldsymbol{\alpha} - (\mathbf{I}_T \otimes \mathbf{I}_S)\boldsymbol{\theta});$$

$$\mathbf{Q}_\delta = \tau_\delta \mathbf{K}_\delta + \tilde{\mathbf{A}}_3' \tilde{\mathbf{A}}_3 = \tau_\delta \mathbf{K}_\delta + n \mathbf{I}_{TS}$$

Centre the sampled values either row wise, column wise or both depending on the type of interaction.

6. Sample the precision parameters $\tau_{\beta_1}, \dots, \tau_{\beta_{D-1}}, \tau_\alpha, \tau_\theta, \tau_\delta$. The full conditionals for these parameters are Gamma, for instance:

$$\tau_\theta | \dots \sim G(a + .5 \times \text{rank}(\mathbf{K}_\theta), b + .5 \times \boldsymbol{\theta}' \mathbf{K}_\theta \boldsymbol{\theta})$$

ACKNOWLEDGEMENTS

We wish to thank Carlo Ferrari, Giovanna Pezzi and Andrea Velli for introducing us to the problem, providing data and performing data pre-processing.
The research work underlying this paper was funded by a FIRB 2012 grant (project no. RBFR12URQJ; title: Statistical modeling of environmental phenomena: pollution, meteorology, health and their interactions) for research projects by the Italian Ministry of Education, Universities and Research.

REFERENCES

Aitchison J (1986) The Statistical Analysis of Compositional Data. Chapman & Hall, London

Albert JH, Chib S (1993) Bayesian Analysis of Binary and Polychotomous Response Data. J Am Stat Assoc 88:669-679

- Bennett LT, Judd TS, Adams MA (2000) Close-range vertical photography for measuring cover changes in perennial grasslands. *J Range Manage* 53:634–641
- Booth DT, Cox SE, Fifield C, Phillips M, Williamson N (2005) Image analysis compared with other methods for measuring ground cover. *Arid Land Res Manag* 19:91–100
- Booth DT, Tueller PT (2003) Rangeland monitoring using remote sensing. *Arid Land Res Manag* 17:455–478
- Council Directive (92/43/CEE) on the conservation of natural habitats and of wild fauna and flora (http://ec.europa.eu/environment/nature/legislation/habitatsdirective/index_en.htm)
- Egozcue JJ, Pawlowsky-Glahn V, Mateu-Figueras G, Barcelo-Vidal C (2003) Isometric logratio transformations for compositional data analysis. *Math Geol* 35: 279–300
- Egozcue JJ, Pawlowsky-Glahn V (2006) Simplicial geometry for compositional data. In Buccianti et al. (eds) *Compositional data analysis in the Geosciences: From theory to practice*. Geological Society, London, Special Publications, 264, pp 145–159
- Fortin MJ, James PMA, MacKenzie A, Melles SJ, Rayfield B (2012) Spatial statistics, spatial regression, and graph theory in ecology. *Spatial Statistics* 1:100–109
- Frühwirth-Schnatter S, Frühwirth R, Held L, Rue H (2009) Improved auxiliary mixture sampling for hierarchical models of non-Gaussian data, *Stat Comput* 19:479–492
- Guisan A, Zimmermann NE (2000) Predictive habitat distribution models in ecology. *Ecol Model* 135:147–186
- Hron K, Filzmoser P, Thompson K (2012) Linear regression with compositional explanatory variables. *J Appl Stat* 39:1115–1128
- Kneib T, Muller J, Hothorn T (2008) Spatial smoothing techniques for the assessment of habitat suitability. *Environ Ecol Stat* 15: 343–364
- Knorr-Held L (2000) Bayesian modelling of inseparable space-time variation in disease risk. *Stat Med* 19:2555–2567
- Kuntz KL, Larson DW (2006) Microtopographic control of vascular plant, bryophyte and lichen communities on cliff faces. *Plant Ecol* 185:239–253
- Latimer AM, Wu S, Gelfand AE, Silander JA Jr (2006) Building Statistical Models to Analyze Species Distributions. *Ecol Appl* 16:33–50
- Lindgren F, Rue H (2008) On the Second-Order Random Walk Model for Irregular Locations. *Scand J Stat* 35:691–700
- Lundholm JT, Larson DW (2003) Relationships between spatial environmental heterogeneity and plant species diversity on a limestone pavement. *Ecography* 6:715–722

- Pueyo Y, Alados CL (2007) Abiotic factors determining vegetation patterns in a semi-arid Mediterranean landscape: Different responses on gypsum and non-gypsum substrates. *J Arid Environ* 69: 490–505
- Otsus M, Zobel M (2002) Small-scale turnover in a calcareous grassland, its pattern and components. *J Veg Sci* 13:199-206
- Richardson MD, Karcher DE, Purcell LC (2001) Quantifying turfgrass cover using digital image analysis. *Crop Sci* 41:1884–1888.
- Rue H, Held L (2005) Gaussian Markov random fields: theory and applications. Chapman & Hall/CRC Press, London.
- Rue H, Martino S (2009) Approximate Bayesian inference for latent Gaussian models by using integrated nested Laplace approximations (with discussion). *J Roy Stat Soc B* 71:319-392
- Rue H, Martino S, Lindgren F, Simpson D, Riebler A (2013) INLA: Functions which allow to perform full Bayesian analysis of latent Gaussian models using Integrated Nested Laplace Approximation. R package version 0.0-1383402327
- Schrödle B, Held L (2011) Spatio-temporal disease mapping using INLA. *Environmetrics* 22:725–734
- Spiegelhalter DJ, Best NG, Carlin BP, Van der Linde A (2002) Bayesian Measures of Model Complexity and Fit (with Discussion). *J Roy Stat Soc B* 64:583-616
- Velli A. (2014) Relationships between plant diversity and environmental heterogeneity in rupicolous grasslands on gypsum. The case study of Alysso-Sedion albi (Habitat 6110). Dissertation, University of Bologna
- Wahba G (1978) Improper priors, spline smoothing and the problem of guarding against model errors in regression. *J Roy Stat Soc B* 40:364–372
- Wikle CK (2003) Hierarchical Bayesian models for predicting the spread of ecological processes. *Ecology* 84:1382-1394.